Charge excitation and the normal-state transport properties in the flux-binding phase of the t-J model

Z.Y. Weng, D.N. Sheng, and C.S. Ting
Texas Center for Superconductivity and Department of Physics, University of Houston, Houston, Texas 77204-5506
(Received 15 March 1994)

Elementary excitations are discussed in the flux-binding phase [Weng, Sheng, and Ting, Phys. Rev. B **49**, 607 (1994)] of the t-J model. It is shown that the density and current constraints in the gauge-theory description will dramatically modify the charge excitations. An effective Lagrangian for the normal state of the flux-binding phase is derived, and based on it the transport properties are studied. We find that the resistivity is linearly temperature dependent with a relaxation rate $\hbar/\tau \simeq 2k_BT$, and the Hall coefficient involves a second relaxation rate with the cotangent Hall angle following a T^2 law. Furthermore, the thermopower exhibits a strong doping dependence. All these features are in good agreement with the transport measurements of the high-T_c copper-oxide compounds.

I. INTRODUCTION

After several years efforts since the discovery of the high-T_c copper oxide superconductors, the experiments now have achieved a great deal of consensus about the anomalous normal-state transport properties in these materials. For example, it is well known that the resistivity in the CuO_2 layers increases linearly in temperature for all the hole-doped compounds in the optimal T_c regime. Combined with the optical measurements,[1] such a temperature dependence of resistivity has been related to a linear-T dependence of the scattering rate $\hbar/\tau \simeq 2k_BT$. A linear-frequency dependence of $\hbar/\tau(\omega)$ at $\omega > T$ has also been implied in the infrared spectroscopy[1] up to 0.15 eV. The Hall measurements show the hole characteristic with a strong temperature anomaly.[2] The recent Hall angle concept proposed by the Princeton group,[3,4] with the involvement of a second scattering rate, has given an excellent account for the temperature dependence as well as the impurity effects.[4] The thermopower in these compounds exhibits[5] a monotonic decrease with increasing doping, and its sign could even change in the overdoped regime.

These transport properties impose a strong constraint on the possible theories of the high-T_c superconductivity. Several strong-correlation-based theories have been developed under the inspiration of the experiments. Among them the gauge-field theory[6-8] for the uniform resonant-valence-bond (RVB) state and Anderson's two-dimensional (2D) Tomonaga-Luttinger liquid theory[9,3] have attracted much attention. Nevertheless a full and systematic understanding of the aforementioned transport properties has not yet been attained within the framework of these approaches.

Recently a so-called flux-binding phase[10] in the 2D t-J model has been investigated. This phase is obtained based on a generalization[11] of the phase-shift phenomenon originally identified in one-dimensional (1D) case.[12] Superconductivity exhibits in the ground state of the flux-binding phase, and the physical origin of such a phase shares some similarities with the gauge theories[13-17] of the commensurate flux phase.[18] In the latter case, the tendency of flux binding (and thus the statistics transmutation) is reflected in the Chern-Simons terms[13,14] appearing in the gauge fluctuations.

The flux-binding phase[10] is composed of three subsystems connected together by the gauge fields. It can be described in terms of a decomposition scheme of electron operator as[10] $c_{i\sigma} = h_i^+(f_{i\sigma}e^{i\theta_i^f})(e^{-i\theta_i^{eo}}e_i)$. Such a decomposition is different from the usual slave-particle scheme[19] by the presence of a third species e_i as well as the nonlocal phases $\theta_i^{f,eo} = \frac{1}{2}\sum_{l\neq i}\mathrm{Im}\ln(z_i - z_l)n_l^{f,eo}$ (where $n_l^{f,eo}$ are the number operators of $f_{l\sigma}$ and e_l species and $z_i = x_i + iy_i$.) The bosonic operator h_i^+ and the fermionic operator $f_{i\sigma}$ are similar to those in the slave-boson formalism.[19] They may be called holon and spinon operators, respectively, just for convenience. Later in this paper we will identify the real charge and spin excitations in the system. The introduction of a bosonic operator e_i, called an eon,[10] in the decomposition is based on the following consideration. It is a well-known fact that the hopping and superexchange processes in the t-J model, both comparable in energy, cannot be simultaneously optimized in the 2D case. In other words, the hopping of holes in a well-correlated spin background will get frustrated, or conversely, the spin correlation has to be suppressed in favor of the hopping of holes. This represents a strong-correlation characteristics of the t-J model. Nevertheless, we still may optimize the saddle-point energies for both h_i^+ and $f_{i\sigma}$ *at the same time*, and then let e_i take care of the frustration effect as a "backflow" of the holon h_i. It turns out[10] that, with the presence of the nonlocal phases $\theta_i^{f,eo}$, three subsystems can simultaneously become the local energy minima

in such a way that the gauge fluctuations around these saddle-points are suppressed. Such a suppression of the gauge fields will lead to a significant simplification in the treatment of the flux-binding phase.

The structure of the flux-binding phase is schematically illustrated by Fig. 1. Three subsystems in Fig. 1 are connected together by the temporal gauge fields, λ and β, which enforce the on-site density constraints

$$n_i^h + n_i^f = 1, \qquad n_i^h + n_i^{eo} = 1, \tag{1.1}$$

and the spatial gauge fields $\boldsymbol{a}^f$ and $\boldsymbol{a}^{eo}$, which give rise to the current constraints

$$\mathbf{J}_h = -\mathbf{J}_f = -\mathbf{J}_{eo}, \tag{1.2}$$

among the holon, spinon, and eon subsystems. The electronic quantities such as number operator n_i^e, current operator $\mathbf{J}_e$ and spin operator $\mathbf{S}_i^e$ are related to these species through $n_i^e = 1 - n_i^h$, $\mathbf{J}_e = \mathbf{J}_h$, and $\mathbf{S}_i^e = \sum_{\sigma\sigma'} f_{i\sigma}^+(\hat{\sigma})_{\sigma\sigma'} f_{i\sigma'}$, etc., where $\hat{\sigma}$ is the conventional Pauli matrix.

In the ground state, the holons as a boson gas are in the Bose condensation. The spinon and eon subsystems, as the results of flux binding, are two semionic systems which also show the Meissner effect.[10] The total response of the whole system to an external electromagnetic field is given by a Ioffe-Larkin combination rule of three subsystems as follows[10]

$$K = \left(\Pi_h^{-1} + \Pi_f^{-1} + \Pi_{eo}^{-1}\right)^{-1}, \tag{1.3}$$

where Π_h, Π_f, and Π_{eo} are the response matrices for the corresponding subsystems. As a result of (1.3), the K matrix exhibits a real superconducting response to an external field. On the other hand, the time-reversal (T) and parity (P) symmetries, which are violated in the spinon and eon subsystems, are restored in the electronic response function K due to the cancellation of the T and P violations between these two degrees of freedom. And such a cancellation has been argued[10] to be generically true as the result of the exactness of the current constraint (1.2) and the topological flux-binding condition. The pairing characteristics in such a superconducting state will be discussed elsewhere.

In the present paper, we will first focus on the elementary excitations in the flux-binding phase. We stress the fact that the decomposition of an electron operator in the present form,[10] or in the usual slave-particle formalism,[19] is more of a mathematical convenience for implementation of the no-double-occupancy constraint than of a real physical one. In fact, Eq. (1.2) implies that neither the spinon $f_{i\sigma}$ only describes the spin degree of freedom nor the holon h_i solely keeps the track of the charge. The real excitations can be dramatically different from the underlying holon, spinon, and eon species, which are confined by the constraints (1.1) and (1.2) in the decomposition formulation. As it will be shown later, the topological characteristics of the spinon and eon subsystems make the construction of the elementary excitations simple and accurate, independent of the detailed approximations. In Sec. II, the independent charge and spin excitations are identified, which indicates the existence of a real charge-spin separation in the flux-binding phase.

Then we discuss the finite temperature properties and find an exotic *normal state* where the elementary excitations will resume rather simple forms. There the Bose condensation of holons is gone, while the spinons and eons still remain condensed in the semionic states. Subsequently, a systematic study of the transport properties for such a normal state are presented. The results can systematically explain the main anomalies found in the high-T_c materials in a very consistent way. This calculation will lend a strong experimental support to the present flux-binding phase. The effective Lagrangian for the charge fluid in such a normal state is derived in Sec. III A. Then the transport properties is studied in Sec. III B. Finally a summary will be presented at the end of the paper.

II. ELEMENTARY EXCITATIONS IN THE FLUX-BINDING PHASE

The effective gauge-theory description of the flux-binding phase, as depicted in Fig. 1, is given by the following Lagrangian[10]

$$\mathcal{L} = \mathcal{L}^0 + \mathcal{L}^1, \tag{2.1}$$

where

$$\begin{aligned}\mathcal{L}^0 = &\sum_i h_i^+ \left[\partial_\tau + a_{0i}^{\mathrm{ext}}\right] h_i + \sum_{i\sigma} f_{i\sigma}^+ \partial_\tau f_{i\sigma} + \sum_i e_i^+ \partial_\tau e_i \\ &+ \sum_i \lambda_i \left(\sum_\sigma f_{i\sigma}^+ f_{i\sigma} + h_i^+ h_i - 1\right) \\ &+ \sum_i \beta_i (e_i^+ e_i + h_i^+ h_i - 1),\end{aligned} \tag{2.2}$$

and $\mathcal{L}^1 = H_h + H_f + H_{eo}$ with

$$H_h = -t_h \sum_{\langle ij\rangle} e^{i(a_{ij}^{\mathrm{ext}} + a_{ij}^f + a_{ij}^{eo})} h_i^+ h_j + \mathrm{H.c.}\,, \tag{2.3a}$$

$$H_f = -J' \sum_{\langle ij\rangle\sigma} e^{i(q_f A_{ij}^f + a_{ij}^f)} f_{i\sigma}^+ f_{j\sigma} + \mathrm{H.c.}\,, \tag{2.3b}$$

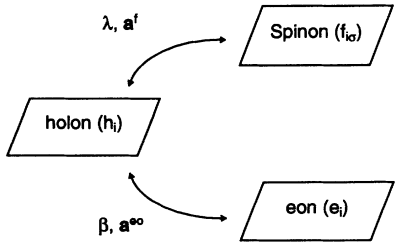

FIG. 1. Three subsystems in the flux-binding phase are connected together by the gauge fields λ, β, $\boldsymbol{a}^f$, and $\boldsymbol{a}^{eo}$.

$$H_{eo} = -t_{eo} \sum_{\langle ij \rangle} e^{i(q_{eo} A_{ij}^{eo} + a_{ij}^{eo})} e_i^+ e_j + \text{H.c.} \qquad (2.3c)$$

In Eq. (2.2), the Lagrangian multipliers λ_i and β_i are introduced to enforce the on-site density constraints (1.1). a_{0i}^{ext} and a_{ij}^{ext} in Eqs. (2.2) and (2.3a) represent the temporal and spatial components of the external electromagnetic fields, respectively.

The "charges" $q_f = -1$ and $q_{e0} = +1$ in Eqs. (2.3b) and (2.3c) and the nonlocal gauge fields $A_{ij}^{f,eo}$ are defined by

$$A_{ij}^{f,eo} = \frac{1}{2} \sum_{l \neq i,j} \text{Im} \ln \left(\frac{z_i - z_l}{z_j - z_l} \right) n_l^{f,eo}, \qquad (2.4)$$

which satisfy the topological relations

$$\sum_C A_{ij}^{f,eo} = \pm \pi \sum_{l \in C} n_l^{f,eo}, \qquad (2.5)$$

where C refers to an arbitrary closed loop on the lattice without crossing and $\pm$ depends on the direction on the loop. Equation (2.5) states the fact[10] that the fictitious fluxes represented by $A_{ij}^{f,eo}$ are all quantized as π flux tubes (in the unit that the flux-quantum $\phi_0 \equiv hc/e$ is equal to 2π) and bound to the spinons and eons, respectively, which is the basic reason for the present state being called as the flux-binding phase.[10] One immediately sees that $A_{ij}^{f,eo}$ play the roles of statistics transmutation[20,21] in the spinon and eon subsystems. H_f can be regarded as describing a semion system with spin index and H_{eo} describing a single species semion gas in the boson representation.

a_{ij}^f and a_{ij}^{eo} in Eqs. (2.3b) and (2.3c) represent the spatial gauge fluctuations around the saddle points characterized by the flux binding gauge fields $A_{ij}^{f,eo}$. If the present flux-binding state is stable, the gauge fields a_{ij}^f and a_{ij}^{eo} should get suppressed in favor of $A_{ij}^{f,eo}$ in Eqs. (2.3b) and (2.3c). That is what has been shown in Ref. 10, where gaps are found in the transverse channel of the gauge fluctuations. Furthermore, the quadratic fluctuations of a_{ij}^f and a_{ij}^{eo} will lead to the local current constraints (1.2). Equation (1.2) manifests the following facts: A forward hopping of a holon h is balanced by a backward hopping of a spinon f and, at the same time, is always accompanied by a backflow of eon e. The constraints (1.1) and (1.2) are the generic consequences of a gauge theory description, which is independent of the detailed approximations in the treatment of the Lagrangian (2.1). Note that the density constraint (1.1) and the longitudinal part of (1.2) are connected with each other by the conservation law $\partial_t \rho + \nabla \cdot \mathbf{J} = 0$. This connection is reflected in the local gauge invariance of the Lagrangian (2.1) (Ref. 10). In general, the longitudinal components of a_{ij}^f and a_{ij}^{eo} can be absorbed into the temporal gauge fields λ_i and β_i through the local gauge transformation. Thus in the present paper, we will always regard the spatial components a_{ij}^f and a_{ij}^{eo} only as the transverse ones without loss of generality.

The dynamics of the gauge fields are generated by coupling to the holons, spinons, and, eons, and, in principle, can be determined by integrating out the degrees of freedom of the latter in the Lagrangian (2.1). The dynamics of each subsystem should be in turn affected by the gauge-field fluctuations. In the gauge theory[6-8] of the uniform RVB state, for example, the gauge interaction turns out to be so strong in the transverse channel that a self-consistent treatment of the whole problem may be crucial. Fortunately, in the flux-binding phase the transverse gauge fluctuations are suppressed,[10] like an external electromagnetic field in a superconductor. So each subsystem will behave independently in the long-wavelength, low-energy regime. However this does not simply mean that the whole system becomes really decoupled. Remember that each subsystem in the ground state is a superfluid condensate which, as a whole, can respond to the gauge fluctuations rather sensitively even if the latter is suppressed. Thus one will find a very peculiar situation later. On the one hand each subsystem can be mathematically treated as independent one, due to the "rigidity"[22] of a superfluid system with regard to an "external" field; on the other hand, the whole system as composed of these subsystems can show totally new behaviors after the constraints (1.1) and (1.2) are imposed via the gauge fields. In the following, we will first discuss the elementary excitations in each individual subsystems and then turn to discuss the real excitations for the whole system.

A. Charge excitations and flux-quantization in a semion gas

The spinon and eon systems described by H_f [Eq. (2.3b)] and H_{eo} [Eq. (2.3c)] are basically the semionic systems, with each particle carrying a half-quantized Bohm-Aharonov flux tube through $A_{ij}^{f,eo}$ defined by Eq. (2.4). Their long-wavelength behaviors have been discussed in Ref. 10 and each of them exhibits the "Meissner effect" as response to the gauge fields $a_{ij}^{f,eo}$, similar to a usual spinless semion gas.[23-25] The latter has been extensively studied in the literature,[21,23-29] and besides the Meissner effect, the charge excitation as a charge-vortex compound has been discussed.[21,26] The flux-quantization has been also argued,[21,27,30] and the demonstration has been given in the exact diagonalizations[31,32] for a lattice semion gas. These general characteristic properties for a semion system are very essential in order to understand the elementary excitations in the present flux-binding phase.

The response functions, Π_f and Π_{eo}, of the spinon and eon subsystems show the following properties[10] at small q and ω

$$\Pi_f(q,\omega) \propto \text{const.}, \quad \Pi_{eo}(q,\omega) \propto \text{const.} \qquad (2.6)$$

Equation (2.6) will lead to the following London equation[10]

$$\mathbf{J} = -\left(\frac{\rho}{m}\right) \boldsymbol{a}, \qquad (2.7)$$

where $\mathbf{J}$ denotes the spinon or eon current and $\boldsymbol{a}$, in the gauge $\nabla \cdot \boldsymbol{a} = 0$, is a corresponding gauge field of $a_{ij}^{f,eo}$ in the continuum limit. A current operator can be written in the following form:

$$\hat{\mathbf{J}} = \hat{\mathbf{J}}^p - q_{f,eo}\frac{\boldsymbol{a}}{m}\psi^+\psi, \tag{2.8}$$

where $\hat{\mathbf{J}}^p$ is the so-called paramagnetic current[22] and the second term on the right is a diamagnetic current with ψ as a spinon or eon field. Comparing (2.8) with (2.7) and noticing $\rho = \langle\psi^+\psi\rangle$ one finds

$$\langle\hat{\mathbf{J}}^p\rangle = 0, \tag{2.9}$$

which implies the rigidity of a semion system and thus the perfect diamagnetism.[23,24] It is noted that Eq. (2.6) has been derived in Ref. 10 by using the continuum approximation. A technique for a lattice semion can be found in Ref. 17, which could give the similar results as Eq. (2.6). A discussion of the lattice effect can also be found in Ref. 33.

The charged vortices has been first discussed in Refs. 21 and 26 as the elementary excitations in a semion gas. Such a charge excitation can be created by adding (particle-like) or extracting (hole-like) a semion. Since a semion is always attached by a fictitious flux tube, a charge excitation as such will then be accompanied by an excess or deficit of a quantized flux $\phi_0/2$. This extra fluxoid will then induce a vortexlike screening current in the semion background according to Eq. (2.7):

$$\mathbf{J} = \pm\left(\frac{\rho}{m}\right)\left(\frac{\phi_0/2}{2\pi}\right)\frac{\hat{\mathbf{z}}\times\mathbf{r}}{r^2}. \tag{2.10}$$

The total energy will then be enhanced by

$$\Delta E = \frac{\rho}{2m}\int d^2\mathbf{r}\ \ \boldsymbol{a}^2 \approx \frac{\rho\phi_0^2}{16\pi m}\ln(R/a_c), \tag{2.11}$$

where a_c is a cutoff scale of the fluxoid and R is the size of the whole system. Thus such a charged vortex has a logarithmic-divergent energy, which was first discussed in Refs. 21 and 26. In a semion system, the charged vortices as the elementary charge excitations will dominate the finite-temperature behaviors and could lead to a Kosterlitz-Thouless-like transition as argued in Ref. 27.

Nonetheless, a finite-energy charge excitation can also exist in a semion system, which is closely related to the flux-quantization effect. Suppose a charge vortex described above is created at the origin. We may let a quantized flux of an external field penetrate through at the same location in order to compensate the excess or deficit flux tube associated to the charged vortex as shown in Fig. 2. For a hole-type excitation, such an external fluxoid has to be parallel to the internal fictitious flux tubes carried by the semions, while for a particle-type excitation, the external fluxoid goes to opposite direction. Then no net diamagnetic current such as (2.10) should be produced to circulate this charge excitation anymore, due to the exact compensation in a scale larger than the sizes of the fluxes. With the absence of this long-range effect, only a finite energy would be needed to create such a *charge-fluxoid* excitation.[27,30]

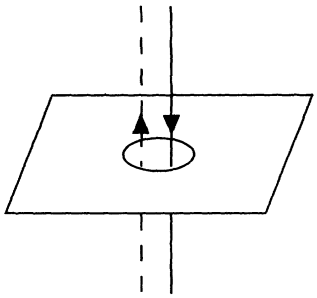

FIG. 2. A charge-fluxoid excitation as a combination of an external flux-quantum (solid arrow) and a charge-vortex excitation with a fictitious flux (dashed arrow).

An estimation of the energy for the charge-fluxoid excitation can be carried out similar to the calculation of the energy for a charged vortex by Hanna, Laughlin, and Fetter.[26] With the extra external flux shown in Fig. 2, the logarithmic-divergent energy will be found being cancelled out.[34] For a variationally constructed excitation, one expects that the excitation energy can be further lowered by adjusting both the size of the external fluxoid and the shape of the local wave function of the charge excitation.

The stability of the charge-fluxoid excitation requires that a net flux or charge could not be added to or moved away from such an excitation. In other words, the stability of a charge-fluxoid excitation is connected to the conditions (a) flux quantization at $\phi_0/2$ of the external fluxoid and (b) a particle or hole (for particle-type or hole-type excitation), which is always bound to the quantized external fluxoid at a local scale. A violation of either condition will lead to a net flux (external or internal) emerging at the location of the excitation. Such an uncompensated flux will then induce a long-range diamagnetic screening current in terms of Eq. (2.7) and would cost a logarithmic energy similar to (2.11). Therefore, in a semion system, the existence of the Meissner effect will sufficiently lead to the flux-quantization of an external field at $\phi_0/2$. And such a flux-quantization is always related to the so-called charge-fluxoid excitation where a charge (either particle or hole) is attached to the external fluxoid. This is consistent with both the mean-field[30] and Chern-Simons field theory[27] considerations.

B. Elementary excitations in the flux-binding phase

For a decoupled system, the excitations could be decided by the individual subsystems. But as already pointed out before, the flux-binding phase is *not* simply decoupled and the existence of the constraints between the subsystems will modify the elementary excitations in a nontrivial way. In the following we will discuss both the charge and spin excitations in such a system.

Charge excitation. Suppose a hole-type *charge-vortex*

excitation is created, say, in the spinon subsystem by removing a spinon at the origin. Because of the density constraint (1.1), a similar hole-type excitation should be simultaneously produced in the eon subsystem as shown by Fig. 3 (i.e., removing an eon at the same location). According to Eq. (2.10), the vortex-like diamagnetic currents surrounding these excitations will behave as

$$\mathbf{J}_{f(eo)} \propto q_{f(eo)} \frac{\phi_0}{4\pi} \frac{\hat{\mathbf{z}} \times \mathbf{r}}{r^2}, \tag{2.12}$$

in the spinon and eon subsystems, respectively. Since $q_f = -q_{eo} = -1$, one finds that the diamagnetic currents of spinons and eons are in opposite directions, i.e., $\mathbf{J}_f \simeq -\mathbf{J}_{eo}$ (cf. Fig. 3), which obviously violates the current constraint (1.2). A similar particle-type excitation has the same problem. Thus the charge-vortex excitations as the elementary charge excitations in a semion gas will *not* be allowed to appear in the flux-binding phase after the constraints (1.1) and (1.2) are imposed. This is an important result for the flux-binding phase. It implies that the finite temperature behaviors of the spinon and eon subsystems will be quite different from an isolated semionic system, in which the charge-vortex composites as the elementary excitations could lead to a Kosterlitz-Thouless transition at a finite temperature.[27]

Recall that the current constraint (1.2) is enforced through the gauge fields $\boldsymbol{a}^f$ and $\boldsymbol{a}^{eo}$. In the case of the charge-vortices discussed above, in order to restore the current restriction (1.2), the fluctuations of $\boldsymbol{a}^f$ and $\boldsymbol{a}^{eo}$ will have to produce two extra fluxoids in opposite directions at the same location of the excitations in the spinon and eon subsystems. These quantized fluxoids will play a role in compensating the deficit fluxes attached to the hole-type charge-vortices shown in Fig. 3 (dashed arrows) so that the vortex-like diamagnetic currents (2.12) are exactly cancelled out as in Fig. 2. Then the current constraint (1.2) will be recovered in a form of $\mathbf{J}^f = \mathbf{J}^{eo} = 0$ at a distance away from the excitation. Obviously the resulting composite is nothing but a compound of the *charge-fluxoid* excitations (cf. Fig. 2) in the spinon and eon subsystems, respectively. Here $\boldsymbol{a}^f$ and $\boldsymbol{a}^{eo}$ can be regarded as the "external" fields for the subsystems (cf. Fig. 1), and in each subsystem a charge (hole) is bound to a quantized external flux produced by the transverse gauge field to form a charge-fluxoid excitation. Thus only the charge-fluxoid excitations in the spinon and eon subsystems survive the constraints (1.1) and (1.2) in the flux-binding phase.

Thus, even though the gauge fields $\boldsymbol{a}^f$ and $\boldsymbol{a}^{eo}$ are usually suppressed[10] in the long-wavelength regime due to the Meissner effect, their short-wavelength fluctuations can still produce quantized fluxes to penetrate the corresponding subsystems, resembling a type-II superconductor. These flux lines are connected to the charge excitations in these semionic subsystems as discussed above. On the other hand, since the fluxoids produced by $\boldsymbol{a}^f$ and $\boldsymbol{a}^{eo}$ are in the opposite direction, their sum $\boldsymbol{a}^f + \boldsymbol{a}^{eo}$, which appears in the holon subsystem [Eq. (2.3a)], will not be changed and thus the holon part is not affected by the excited fluxoids. Nonetheless, when a pair of hole-type charge-fluxoid entities are excited in the spinon and eon subsystems, a holon has to be simultaneously added to the same location in terms of the density constraint (1.1). Then a real hole is created in the present flux-binding phase as a composite excitation schematically shown in Fig. 4, where p, q, and h specify the hole-type components in the spinon, eon, and holon subsystems, respectively, and are bound together in real space through some Lagrangian multipliers $\tilde{\lambda}$ and $\tilde{\beta}$ which will be introduced in Sec. III.

Effective Hamiltonians of p and q species can be determined as follows. Let us consider a p species first. According to the definition, the p species is a hole-type charge-fluxoid excitation in the spinon subsystem described by the Hamiltonian (2.3b). If we move a p species slowly to go through a closed path C in real space, the corresponding Berry phase Φ_C is found equal to the total fluxes enclosed in the loop as seen by the charge attached to such a p species. That is

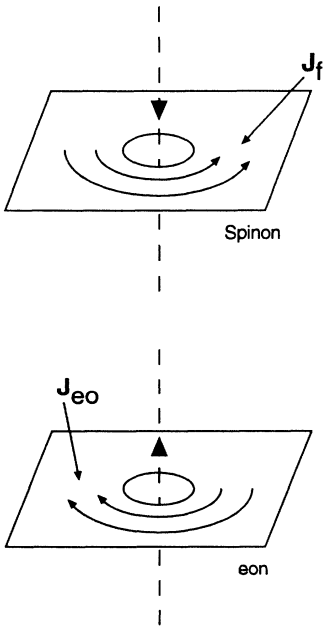

FIG. 3. A pair of the charge-vortex excitations in the spinon and eon subsystems.

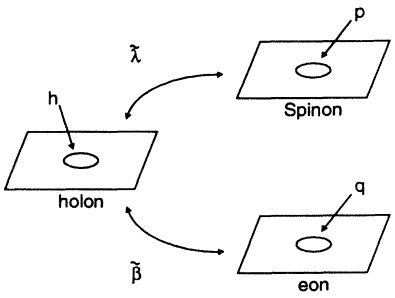

FIG. 4. A real charge excitation is schematically shown as a composite particle of the exciations h, p, q in the three subsystems.

$$\Phi_C = -\int_C d\mathbf{r}\cdot(q_f\mathbf{A}^f + \boldsymbol{a}^f) \equiv \int_C d\mathbf{r}\cdot\mathbf{A}^p, \qquad (2.13)$$

where a continuum limit is taken because p is an entity with a size comparable to the lattice spacing and thus the phase counting becomes meaningless when a loop is as small as, say, a plaquette. $\mathbf{A}^f$ in Eq. (2.13) as a continuum version of A^f_{ij} [cf. Eq. (2.4)] is given by

$$\mathbf{A}^f = \frac{1}{2}\int d^3\mathbf{r}\frac{\hat{\mathbf{z}}\times(\mathbf{r}-\mathbf{r}')}{|\mathbf{r}-\mathbf{r}'|^2}\rho^f(\mathbf{r}')\ , \qquad (2.14)$$

where $\rho^f(\mathbf{r})$ is the spinon density. $\boldsymbol{a}^f$, as a continuum version of a^f_{ij}, can be rewritten in the following form:

$$\boldsymbol{a}^f = \tilde{\boldsymbol{a}}^f + q_f\boldsymbol{a}^f_{\rm ex}, \qquad (2.15)$$

where $\tilde{\boldsymbol{a}}^f$ describes the usual long-wavelength fluctuation, which is gapped and thus suppressed as long as the background spinons remain condensed.[10] $\boldsymbol{a}^f_{\rm ex}$ in Eq. (2.15) describes the short-wavelength fluctuations—quantized fluxes bound to the charge excitations (of both hole and particle types):

$$\boldsymbol{a}^f_{\rm ex} = \frac{1}{2}\int d^3\mathbf{r}\frac{\hat{\mathbf{z}}\times(\mathbf{r}-\mathbf{r}')}{|\mathbf{r}-\mathbf{r}'|^2}[\rho_p(\mathbf{r}')-\tilde{\rho}_p(\mathbf{r}')], \qquad (2.16)$$

in which $\rho^p(\mathbf{r}) = p^+(\mathbf{r})p(\mathbf{r})$, and $\tilde{\rho}^p(\mathbf{r})$ represents the density for the particle-type excitations. Therefore a p species will always see a fictitious vector potential $\mathbf{A}^p$ in real space and the effective Hamiltonian can be written as

$$H_p = \int d^2\mathbf{r}\, p^+(\mathbf{r})\frac{(-i\nabla-\mathbf{A}^p)^2}{2m_p}p(\mathbf{r}), \qquad (2.17)$$

with

$$\mathbf{A}^p = \mathbf{A}^f - \tilde{\boldsymbol{a}}^f + \boldsymbol{a}^f_{ex}. \qquad (2.18)$$

The effective mass m_p for the p species is of the same order of magnitude as the spinon's, which is equal to $(2J'a^2)^{-1}$.

Similarly the effective Hamiltonian for the q species is given by

$$H_q = \int d^2\mathbf{r}\, q^+(\mathbf{r})\frac{(-i\nabla-\mathbf{A}^q)^2}{2m_q}q(\mathbf{r})\ , \qquad (2.19)$$

with $m_q \simeq (2t_{eo}a^2)^{-1}$ and $\mathbf{A}^q = -\mathbf{A}^{eo}-\tilde{\boldsymbol{a}}^{eo}-\boldsymbol{a}^{eo}_{ex}$, where $\mathbf{A}^{eo}$, $\tilde{\boldsymbol{a}}^{eo}$, and $\boldsymbol{a}^{eo}_{ex}$ are the counterparts of $\mathbf{A}^f$, $\tilde{\boldsymbol{a}}^f$, and $\boldsymbol{a}^f_{ex}$ in the eon subsystem.

One can similarly construct the particle-type charge excitations. In contrast to a fractional quantum Hall problem, a semion gas is a compressible system. In such a system, the hole-type and particle-type excitations can be excited separately. However, the density constraint (1.1) will put strong restriction on the particle-type excitations. When a particle-type charge-fluxoid excitation is created in the spinon or eon subsystem, the size of the extra particle has to be large in order to satisfy the on-site constraint (1.1), which requires that the total on-site particle number does not exceed one. As the background particle occupation is already close to each site-one particle at small doping, the wave packet of the particle excitation has to expand to a much larger space on the lattice than a hole-type excitation, which means that the higher Landau levels will be involved in the former, and thus there will be a higher excitation energy. One can imagine that with the increase of temperature more hole-type excitations are thermally produced, and thus in the p- or q-absent regions the background particle occupation should be closer to half filling as a result of particle number conservation. As a consequence, the particle-type excitations become harder to achieve in these regions.

Spin excitation. In the above discussions, the spin degree of freedom in the spinon subsystem has not been touched yet. A quantized fluxoid produced by the gauge field $\boldsymbol{a}^f$ will expel (hole type) or give rise to an accumulation (particle type) of the background spinons to form a spinless charge-fluxoid excitation. These spinless characteristics are a result of the fact that each spinon always carries the same fictitious flux-tube defined in (2.4) no matter what its spin state is.

On the other hand, a spin excitation in the spinon subsystem will not involve a change in the density of particles. Thus there will not be any change in the distribution of the fictitious fluxes, which are bound to the particles and whose long-range effects determine the semionic characteristics. Hence the spin degree of freedom will not involve the topological long-range correlation in contrast to the charge part. Furthermore, a spin process always corresponds to $\mathbf{J}_f = 0$. Without changing both the density and current, a spin excitation will thus not directly affect the eon and holon subsystems through the constraints (1.1) and (1.2). So one expects a relatively simple behavior for the spin degree of freedom in the flux-binding phase, which is solely determined by the spinon subsystem.

If the ground state of the spinon subsystem is described by a mean-field version where the lowest Landau level (with spin degree) is filled,[10] then a spin flip process is represented by a particle-hole excitation across the Landau levels, which does not change the density and local fluxes, and thus does not lead to a diamagnetic current in the background. The spin excitation spectrum will open a gap, which is equal to the Landau gap, in such a continuum limit. But this gap can be reduced after the lattice effect is included in the lattice model (2.3b). Beyond the mean-field approximation, the statistics vector potential A^f_{ij} in (2.4) will fluctuate with the superfluid density and a^f_{ij} will fluctuate with the density of the charge excitations. These fluctuations of the fictitious magnetic fields can lead to a broadening of the spin spectrum and a renormalized spin gap. Such a spin gap will be closed in the normal state. The details of the spin dynamics beyond the mean-field approximation will be discussed elsewhere.

III. NORMAL STATE OF THE FLUX-BINDING PHASE

In Sec. II, we have identified the elementary charge and spin excitations in the flux-binding phase. We have seen how dramatically the constraints have modified the charge excitations. As shown in Sec. II, the holon, eon, and spinon subsystems defined in the decomposition scheme are not directly connected to the physical charge and spin degrees of freedom. A real charge excitation is found to be a composite object composed of the spinless elementary excitations in these subsystems. On the other hand, the spin excitation, without involving charge and current effects, is solely related to the spinon subsystem as one would have expected. In the present section, we will proceed to go to a higher temperature regime where a rather simple structure manifests at the normal state of the flux-binding phase.

With increase of temperature the hole-type charge excitations will get more and more excited. At a critical temperature where the number of those excitations becomes comparable to the total holon number in the system, the residual holons staying at $\mathbf{k}=0$ state will no longer be sufficient to sustain the Bose-condensation in the holon subsystem. (Here we have assumed that the original superfluidity temperature for the holon subsystem is much higher[7] than such a critical temperature.) Then the holon subsystem will experience a normal state transition, which can simultaneously lead to the superfluid-normal state transition of the flux-binding phase even though the spinon and eon subsystems still remain condensed. This point can be clearly seen in terms of Eq. (1.3), where $\Pi_h \to 0$ at small ω when the holon subsystem becomes a normal fluid, and thus $K \propto \Pi_h \to 0$ in this limit, which means the disappearance of the Meissner effect for the whole system.

When the temperature is raised further beyond such a critical temperature, all holons will get excited, as a component of the hole-type charge excitation described in Fig. 4. Then no more charge excitations will be possible beyond the total number of the doped holes. In such a normal state, the particle-type charge excitation can not be excited due to the density constraint. Thus the hole-type charge excitations with a fixed number equal to that of the doped holes will decide the charge degree of freedom in the normal state. These charge excitations can be properly called the renormalized holons and will solely determine the transport phenomena. Since the total numbers of p and q excitations in the spinon and eon subsystems are also fixed at such a hole number, and no other charge excitations are allowed in these subsystems, one expects that the superfluid condensations in the spinon and eon subsystems will be sustained up to quite a wide temperature regime, which are crucial for the present discussion of the normal state being valid.

A. Effective Lagrangian for the charge degree of freedom

For the composite hole-type excitation shown in Fig. 4, the constituent species h, p, and q are bound together as discussed in Sec. II B. In the normal state with all the holons excited, such a binding condition corresponds to

$$h^+(r)h(r) = p^+(r)p(r) = q^+(r)q(r), \tag{3.1}$$

which states the fact that the local densities of h, p, and q are always equal. Obviously Eq. (3.1) must hold at a length scale larger than the sizes of p and q excitations. Inside the p and q species, the situation will become more complicated, which we shall not discuss. Here p and q are interpreted as the "holes" in the spinon and eon subsystems, respectively, and Eq. (3.1) is a natural manifestation of Eq.(1.1) at such a scale. Correspondingly, in the spinon and eon subsystems, one also has the following local-density relations:

$$\rho^p(\mathbf{r}) + \rho^f(\mathbf{r}) = \frac{1}{a^2}, \tag{3.2a}$$

$$\rho^q(\mathbf{r}) + \rho^{eo}(\mathbf{r}) = \frac{1}{a^2}, \tag{3.2b}$$

which can be obtained by combining the continuum version of Eq. (1.1) with Eq. (3.1).

In terms of Eq. (3.2a), the vector potential $\mathbf{A}^p$ [Eq. (2.18)] seen by the p species is reduced to

$$\mathbf{A}^p = \mathbf{A} - \tilde{\boldsymbol{a}}^f, \tag{3.3}$$

with

$$\mathbf{A} = \frac{H}{2}\hat{\mathbf{z}} \times \mathbf{r}, \tag{3.4}$$

which corresponds to a uniform fictitious magnetic field

$$H = \frac{\phi_0}{2a^2}. \tag{3.5}$$

Similarly $\mathbf{A}^q$ seen by the q species becomes

$$\mathbf{A}^q = -\mathbf{A} - \tilde{\boldsymbol{a}}^{eo}. \tag{3.6}$$

Therefore, in the present normal state where Eqs. (3.2a) and (3.2b) hold, the total background fictitious fluxes become uniformly distributed as described by Eq. (3.5).

By incorporating Eqs. (3.1), (2.17), (2.19), and (2.3a), an effective Lagrangian for the charge degree of freedom in the normal state of the flux-binding phase can be then written down as follows:

$$\mathcal{L}_n = \mathcal{L}_n^0 + \mathcal{L}_n^1, \tag{3.7a}$$

with

$$\mathcal{L}_n^0 = \int d^2\mathbf{r}\{h^+[\partial_\tau + a_0^h - (\tilde{\lambda}+\tilde{\beta})]h + p^+[\partial_\tau + a_0^p + \tilde{\lambda}]p + q^+[\partial_\tau + a_0^q + \tilde{\beta}]q\}, \tag{3.7b}$$

$$\mathcal{L}_n^1 = \int d^2\mathbf{r}\left\{h^+\frac{(-i\nabla - \boldsymbol{a}^{\mathrm{ext}})^2}{2m_h}h + p^+\frac{(-i\nabla - \mathbf{A})^2}{2m_p}p + q^+\frac{(-i\nabla + \mathbf{A})^2}{2m_q}q\right\}, \tag{3.7c}$$

where the effective mass approximation has been applied to the holon part in (3.7c) with $m_h = (2t_h a^2)^{-1}$.

In Eq. (3.7b), the Lagrangian multipliers $\tilde{\lambda}$ and $\tilde{\beta}$ are introduced to implement the density constraint (3.1). As a minimum length scale for Eq. (3.1) to hold is the size of the p and q species, which may be approximated by the magnetic length $a_0 = H^{-1/2}$, an ultraviolet cutoff $q_c \sim 1/a_0$ in the momentum space of the $\tilde{\lambda}$ and $\tilde{\beta}$ fields in (3.7b) should be kept in mind. The temporal component of the external electromagnetic field $a_0^{\rm ext} \equiv a_0^h + a_0^p + a_0^q$ is distributed in the three subsystems through a_0^h, a_0^p, and a_0^q in (3.7b) in such a way to make the longitudinal part of the current constraint (1.2) satisfied. Note that $\mathbf{J}_f^l = -\mathbf{J}_p^l$ and $\mathbf{J}_{eo}^l = -\mathbf{J}_q^l$ in the normal state as a result of the charge conservation law $\partial_t \rho + \nabla \cdot \mathbf{J}^l = 0$ for each subsystem, where the subscript l represents the longitudinal component. In fact, one can easily show that due to the presence of the temporal gauge fields $\tilde{\lambda}$ and $\tilde{\beta}$ (which can be transformed into the longitudinal spatial gauge fields after a gauge transformation), the following current constraint always holds (at a scale larger than q_c^{-1}):

$$\mathbf{J}_h^l = \mathbf{J}_p^l = \mathbf{J}_q^l. \tag{3.8}$$

On the other hand, since both the spinon and eon backgrounds are still condensed, the long-wavelength transverse gauge fluctuations $\tilde{\boldsymbol{a}}^f$ and $\tilde{\boldsymbol{a}}^{eo}$ are gapped[10] and thus their effects on the dynamics of h, p, and q species are neglected in (3.7). As a consequence, the transverse external electromagnetic field $\boldsymbol{a}^{\rm ext}$ is only applied to the h species in (3.7c). Physically one may attribute this to the fact that the transverse electromagnetic field is excluded from the spinon and eon subsystems due to the Messner effect in the latter subsystems. Neglecting the contributions of $\tilde{\boldsymbol{a}}^f$ and $\tilde{\boldsymbol{a}}^{eo}$ to (3.7c) also means a decoupling of the charge degrees of freedom from the spinon and eon background. The latter from now on will become invisible except for the spin excitations in the spinon subsystem. Thus one has a real charge-spin separation here.

With the absence of the transverse spatial gauge fields in (3.7c), there will be no constraint like (3.8) holding for the transverse currents of p, q, and h. In fact, this is generally true even if one retains the transverse spatial gauge fields $\tilde{\boldsymbol{a}}^f$ and $\tilde{\boldsymbol{a}}^{eo}$ in (3.7), which should be also coupled to the superfluid backgrounds. Notice that the total transverse currents for spinon and eon subsystems are composed of two terms as $\mathbf{J}_f^{\rm tr} = \tilde{\mathbf{J}}_f^{\rm tr} - \mathbf{J}_p^{\rm tr}$ and $\mathbf{J}_{eo}^{\rm tr} = \tilde{\mathbf{J}}_{eo}^{\rm tr} - \mathbf{J}_q^{\rm tr}$, respectively, where $\tilde{\mathbf{J}}_f^{\rm tr}$ and $\tilde{\mathbf{J}}_{eo}^{tr}$ are the superfluid components from the condensed spinon and eon backgrounds. This is in contrast with the longitudinal components where $\tilde{\mathbf{J}}_f^l = \tilde{\mathbf{J}}_{eo}^l = 0$ as noted before. The transverse gauge fields $\tilde{\boldsymbol{a}}^f$ and $\tilde{\boldsymbol{a}}^{eo}$ will then lead to the constraint (1.2) for the transverse component: $\mathbf{J}_h^{\rm tr} = -\mathbf{J}_f^{\rm tr} = -\mathbf{J}_{eo}^{\rm tr}$. In order to balance a finite transverse current $\mathbf{J}_h$, a fictitious transverse electric field with an infinitesimal strength will be sufficient to produce the backflow in the superfluid part of the spinon or eon subsystem to satisfy such a current constraint. On the other hand, such a field has negligible effect on the normal fluid — p and q species.

Finally, we remark on the statistics of the h, p, and q species in the Lagrangian (3.7). From the construction, one easily sees that h and q should be the hard-core bosons, while p is a fermion as inherited from their parent subsystems. Nevertheless, these three species always have to be bound together locally to form a real hole-type excitation, and there is no real physical meaning for each individual of them. When two hole-type excitations are well separated in space, interchanging one component, say, the h species, between them is physically meaningless unless the whole objects are interchanged, which exhibits the fermionic statistics. On the other hand, when two hole-type objects are sufficiently close, the interchange of each species becomes possible where their hard-core characteristics will show up. This suggests that all the h, p, and q species may be equivalently treated as the spinless fermions to avoid the difficulty associated with the hard-core condition in the boson representation. We note that all the qualitative behaviors of transport discussed in the following will not be affected by this statistics transmutation.

B. The normal-state transport properties

A physical interpretation of the effective Lagrangian (3.7) is given below. The original strong charge-spin coupling in the t-J model is now described by a simple model in which a holon h has always to drag the p and q species to move together. In other words, p and q species, which are confined in the lowest Landau level (LLL), represent the spin frustration effect on the doped holes. (For example, a q species is an excitation in the eon subsystem. As already explained in the Introduction, the eon degree of freedom introduced in Ref. 10 describes an additional frustration to the hole's hopping due to the flux-binding effect, which enhances the spin correlation.) The individual p or q has no independent physical meaning, since it always has to be bound to h through the temporal gauge fields $\tilde{\lambda}$ or $\tilde{\beta}$ in (3.7). On the other hand, the holon h can be regarded as carrying the real charge, which couples to the external electromagnetic field in the Lagrangian (3.7) and its current is equal to the measurable electron current

$$\mathbf{J}_h = \mathbf{J}_e, \tag{3.9}$$

which connects the Lagrangian (3.7) to the observable electronic properties.

The temporal gauge fields $\tilde{\lambda}$ and $\tilde{\beta}$ in the Lagrangian (3.7) will play two essential roles: the binding forces among h, p, and q species at a length scale larger than q_c^{-1} and the scattering forces among them in the long-wavelength, low-energy regime. The dynamics of the long-wavelength gauge fluctuations can be determined in the standard way[6,7] by integrating out the quadratic h, p, and q fields in the Lagrangian (3.7). The propagators $D^{\tilde{\lambda}} = -\langle \delta\tilde{\lambda}\delta\tilde{\lambda}\rangle$ and $D^{\tilde{\beta}} = -\langle \delta\tilde{\beta}\delta\tilde{\beta}\rangle$, with $\delta\tilde{\lambda} = \tilde{\lambda} - \mu_p$ and $\delta\tilde{\beta} = \tilde{\beta} - \mu_q$ where μ_p and μ_q, respectively, are the chemical potentials for p and q species, are given by

$$D^{\tilde{\lambda}(\tilde{\beta})}(q,\omega) = -[(\Pi_h^{-1} + \Pi_{q(p)}^{-1})^{-1} + \Pi_{p(q)}]^{-1}. \quad (3.10)$$

$\Pi_{h(p,q)}$ is the density-density correlation function for h (p, q) species. Π_h for a 2D gas is typically of order of $1/t_h$, whereas Π_p and $\Pi_q \sim (k_BT)^{-1}$ as will be demonstrated below. Since we are interested in the temperature range of $k_BT \equiv \beta^{-1} \ll t_h$, we shall then approximate

$$D^{\tilde{\lambda},\tilde{\beta}} \simeq -1/\Pi_{p,q}, \quad (3.11)$$

in the rest of the paper.

To decide the polarization function $\Pi_{p,q}$, we first note that the p and q species stay in the LLL. Define $\gamma_{s'sq} \equiv \sum_k \langle s'|k+q\rangle\langle k|s\rangle$, where $|k\rangle$ is an eigenstate for a free-particle, and $|s\rangle$ refers to the degenerate states in the LLL with the quantum number s specifying the center of the cyclotron orbital. Then the "bubble" diagram contribution $\Pi_p = \beta^{-1}\sum|\gamma|^2 G^p G^p$ from the p species can be written down in real frequency as follows:

$$\Pi_p^R(q,\omega) = \sum_{s's}|\gamma_{s'sq}|^2 \int_{-\infty}^{\infty} \frac{d\omega' d\omega''}{(2\pi)^2} \frac{f(\omega') - f(\omega'')}{\omega + \omega' - \omega'' + i0^+} \times \rho^p(s,\omega')\rho^p(s',\omega''), \quad (3.12)$$

where $f(\omega) = 1/(e^{\beta\omega}+1)$ and ρ^p is the spectral weight function of the p-particle Green's function G^p

$$G^p(s,i\omega_n) = \int_{-\infty}^{\infty} \frac{d\omega'}{2\pi} \frac{\rho^p(s,\omega')}{i\omega_n - \omega'}. \quad (3.13)$$

If there is no broadening in the Landau level, i.e., $\rho^p(s,\omega) = 2\pi\delta(\omega - \omega_0^p)$, where $\omega_0^p = \frac{1}{2}\omega_c^p - \mu_p$ with $\omega_c^p = H/m_p$ as the cyclotron frequency, then (3.12) would show $\Pi_p^R(q,\omega) = 0$ for $\omega \neq 0$. The same also happens to Π_q^R. According to (3.10) or (3.11), however, $D^{\tilde{\lambda},\tilde{\beta}}$ would thus become divergent at $|\omega| > 0$. Coupling to such strong fluctuations of $D^{\tilde{\lambda},\tilde{\beta}}$ in (3.7) would force the Landau levels of p and q broadened. This procedure, of course, has to be treated in a self-consistent way by inserting a broadening $\Gamma_p(s,\omega)$ for ρ_p:

$$\rho^p(s,\omega) = \frac{2\Gamma_p(s,\omega-\omega_0^p)}{\Gamma_p^2(s,\omega-\omega_0^p) + (\omega-\omega_0^p)^2}. \quad (3.14)$$

Substituting (3.14) into (3.12) and rescaling all the internal frequencies in the integrations by $\omega' - \omega_0^p = \xi'\beta^{-1}$, etc., and $\omega = \xi\beta^{-1}$, one may determine Π_p^R and thus the spectral function $P^{\tilde{\lambda}}(q,\omega) = -2\,\mathrm{Im}D^{\tilde{\lambda}}(q,\omega)$ in terms of (3.11). It can be easily shown

$$P^{\tilde{\lambda}}(q,\xi\beta^{-1}) = \frac{2}{\Lambda(q)\beta}\mathrm{Im}\,[F(\xi,\beta\omega_0^p,[\eta])]^{-1}, \quad (3.15)$$

in which F is a function of the dimensionless variables ξ and $\beta\omega_0^p$ as well as a functional of the function

$$\eta(\xi) \equiv \beta\Gamma_p(\xi\beta^{-1}). \quad (3.16)$$

That is,

$$F(\xi,\beta\omega_0^p,[\eta]) = \int\int \frac{d\xi' d\xi''}{(2\pi)^2} \frac{1}{\xi + \xi' - \xi'' + i0^+} \times \left[\frac{1}{e^{\xi'+\beta\omega_0^p}+1} - \frac{1}{e^{\xi''+\beta\omega_0^p}+1}\right] \times \frac{4\eta(\xi')\eta(\xi'')}{[\eta^2(\xi') + \xi'^2][\eta^2(\xi'') + \xi''^2]}. \quad (3.17)$$

By assuming Γ_p is independent of the quantum number s of the LLL (see discussion below), the momentum dependence of $P^{\tilde{\lambda}}$ is solely decided by $\Lambda(q)$ in (3.15) as (Appendix A):

$$\Lambda(q) = \sum_{s,s'}|\gamma_{s'sq}|^2 = \frac{1}{2\pi a_0^2} e^{-\frac{a_0^2 q^2}{2}}, \quad (3.18)$$

whose q dependence become negligible in the long-wavelength regime $q \ll q_c$.

Next we need to calculate the self-energy of the p particle due to scattering with $D^{\tilde{\lambda}}$ and determine the broadening $\Gamma_p(\omega) = -\mathrm{Im}\Sigma^p(\omega)$ self consistently. Without including the vortex correction, $\mathrm{Im}\Sigma_R^p$ in the spectral representation of G^p and D^{λ} can be expressed by

$$\mathrm{Im}\Sigma_R^p(s,\omega) = -\frac{1}{2}\sum_{qs'}|\gamma_{s'sq}|^2 \int \frac{d\Omega}{2\pi}[n(\Omega) + f(\omega+\Omega)] \times \rho_p(\omega+\Omega)P^{\lambda}(q,\Omega), \quad (3.19)$$

in which $n(\Omega) = (e^{\beta\Omega}-1)^{-1}$. The chemical potential in ω_0^p is decided by equation

$$\delta = \frac{1}{N}\sum_s \int \frac{d\omega}{2\pi}\rho_p(s,\omega)f(\omega). \quad (3.20)$$

Again we may rescale the frequency ω by $\omega - \omega_0^p = \xi\beta^{-1}$, and $\Omega = \xi'\beta^{-1}$ in Eqs. (3.19) and (3.20). Equation (3.19) can be rewritten in terms of (3.15) and (3.16) as

$$\eta(\xi) = D_0 \int_{-\infty}^{\infty} \frac{d\xi'}{2\pi}\left[\frac{1}{e^{\xi'}-1} + \frac{1}{e^{\xi+\xi'+\beta\omega_0^p}+1}\right] \frac{2\eta(\xi+\xi')}{\eta^2(\xi+\xi') + (\xi+\xi')^2}\mathrm{Im}F^{-1}(\xi',\beta\omega_0^p,[\eta]). \quad (3.21)$$

Equations (3.17) and (3.21) show that $\eta(\xi)$ depends only on $\beta\omega_0^p$, which is, according to Eq. (3.20) (after the rescaling), a temperature-independent quantity decided only by doping concentration. D_0 in (3.21) is defined by

$$D_0 = \sum_{qs'}\frac{|\gamma_{s'sq}|^2}{\Lambda(q)}. \quad (3.22)$$

D_0 could have a weak s dependence, which would lead

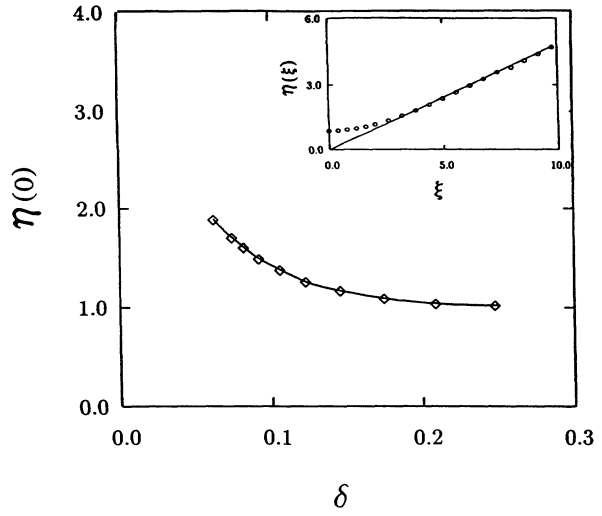

FIG. 5. The coefficient $\eta(0)$ in Eq. (3.23) (square) as a function of the doping concentration δ. The inset shows a curve of $\eta(\xi)$ (circle) vs ξ at $\beta\omega_0^p = 0$.

to a similar s dependence in Γ_p. But since the quantum number s represents the center of the cyclotron orbital here, the dependence of s in D_0 and thus in Γ should not be important as required by the translational invariance. Then one may write

$$D_0 \simeq 2/N \sum_{s'sq} |\gamma_{s's q}|^2/\Lambda(q) = (q_c a_0)^2/2.$$

Therefore in the self-consistent scheme described above, η is a dimensionless function independent of both temperature as well as the coupling strength. Then at $\xi = 0$, one immediately finds

$$\Gamma_p(0) = \eta(0) k_B T, \tag{3.23}$$

from (3.16). Namely, $\Gamma_p(0)$ is always linear in temperature dependence. A solution of $\eta(\xi)$ for Eqs. (3.17), (3.20), and (3.21) can be obtained numerically. The coefficient $\eta(0)$ has a weak-doping dependence as shown in Fig. 5. A typical curve of $\eta(\xi)$ as a function of ξ $(= \beta\omega)$ is also presented in the inset of Fig. 5, which is approximately linear in ξ for $|\xi| > 1$, or equivalently, $\Gamma_p(\omega) \propto |\omega|$ at $|\omega| > k_B T$ according to (3.16). A similar result holds for the q species. One may easily check that $\Pi_{p,q} \propto \beta$, which has been used to justify (3.11). Only in the limit $\delta \to 0$, would the coefficients become so small that the condition requiring that $\Pi_{p,q}$ dominates over Π_h is no longer valid. In this case, one needs to retain all of the contributions from $\Pi_{p,q,h}$ in (3.10). Then $\Gamma_{p,q}(0)$ could deviate from the linear-T dependence.

The relaxation rates $\hbar/\tau_{p,q}$ for p and q species due to scatterings with the gauge fluctuations should be obtained by inserting the vertex correction in the self-energies such as (3.19), which can be reduced to the well-known $1-\cos\theta$ factor[6] in the quasielastic case. But since $D^{\tilde{\lambda},\tilde{\beta}}(q,\Omega)$ have very weak q dependence, $\cos\theta$ essentially has no important effect and $\hbar/\tau_{p,q} \simeq 2\Gamma_{p,q}$. As $\tau_q \approx \tau_p$, one can use a single relaxation time τ_s $(\equiv \tau_p \simeq \tau_q)$ to represent them later:

$$\frac{\hbar}{\tau_s(\omega)} = \begin{cases} 2\eta(0) k_B T, & |\omega| < \beta^{-1} \\ \propto |\omega|, & |\omega| \gg \beta^{-1} \end{cases} . \tag{3.24}$$

The transport relaxation rate $\hbar/\tau_h$ for the h species can be also calculated from scattering with D^{λ} and D^{β}. One can easily write down

$$\mathrm{Im}\Sigma_R^h(k,\xi_k) = -\frac{1}{2}\sum_q [n(\xi_{k+q}-\xi_k) + f(\xi_{k+q})]\left[P^{\tilde{\lambda}}(q,\xi_{k+q}-\xi_k) + P^{\tilde{\beta}}(q,\xi_{k+q}-\xi_k)\right], \tag{3.25}$$

where $\xi_k = k^2/(2m_h) - \mu_h$. At $\xi_k = 0$, the dominant contribution will come from $|\xi_{k+q}| < \beta^{-1}$ on the right-hand side of (3.25), which implies $q \ll q_c$. Since one can neglect the q dependence of $P^{\tilde{\lambda}}$ and $P^{\tilde{\beta}}$ in the long-wavelength regime, one gets

$$\mathrm{Im}\Sigma_R^h(k,0) = -D_h \int d\Omega [n(\Omega) + f(\Omega)][P^{\lambda}(\Omega) + P^{\beta}(\Omega)], \tag{3.26}$$

where the density of states $D_h = m_h a^2/(2\pi)$. A rescaling of the frequency Ω on the right-hand side of the above equation leads to $\mathrm{Im}\Sigma^h(0) = -\eta'(k_B T)^2/t_h$. The numerical value of η' is found ~ 4 with a weak doping dependence. Due to the weak q dependence of $P^{\tilde{\lambda}}$ and $P^{\tilde{\beta}}$, the $1-\cos\theta$ factor will not play a role and one simply has

$$\frac{\hbar}{\tau_h} = -2\,\mathrm{Im}\Sigma_R^h(0) = 2\eta' \frac{(k_B T)^2}{t_h}. \tag{3.27}$$

Resistivity. Apply the external electric field $\boldsymbol{\epsilon} = -\nabla a_0^{\mathrm{ext}}$, with the transverse component $\boldsymbol{a}^{\mathrm{ext}} = 0$. As explained below (3.7), $\boldsymbol{\epsilon}$ will not only act on the holon part but also on the p and q species through a redistribution of the field

$$\boldsymbol{\epsilon} = -\nabla a_0^h - \nabla a_0^p - \nabla a_0^q$$

$$\equiv \boldsymbol{\epsilon}_h + \boldsymbol{\epsilon}_p + \boldsymbol{\epsilon}_q, \tag{3.28}$$

such that the longitudinal current constraint (3.8) holds.

For the h species, the Drude formula of the resistivity is given by $\rho_h = \frac{m_h}{e^2 n \tau_h}$, where n is the density of hole, and then

$$\boldsymbol{\epsilon}_h = \rho_h \mathbf{J}_h^l. \tag{3.29}$$

By the usual procedure, one would also treat the transports of p and q species separately and then combine all of them together by a Larkin-Ioffe-like rule to satisfy the current constraint (3.8) at a *macroscopic* level. However, as the p and q species are subjected to the fictitious magnetic fields, their wave packet sizes are comparable to the magnetic cyclotron length a_0, which is much smaller than the average distance between the composite holes at small doping. Then during the relaxation time before they encounter other composite holes, two wave packets of p and q will have to be bound together *microscopically* in terms of the density constraint (3.1). Since the p and q species see their fictitious magnetic fields in different directions in (3.7), the transverse effects, which would otherwise lead to the Hall effect for each of them, will thus be cancelled out at a length scale larger than $q_c^{-1} \sim a_0$ through the binding force enforced by $\tilde{\lambda}$ and $\tilde{\beta}$.

Thus the $\tilde{\lambda}$ and $\tilde{\beta}$ fields can be effectively divided into two parts,

$$\tilde{\lambda} = \tilde{\lambda}_{\rm scatt} + \tilde{\lambda}_b, \qquad \tilde{\beta} = \tilde{\beta}_{\rm scatt} + \tilde{\beta}_b, \tag{3.30}$$

where $\tilde{\lambda}_{\rm scatt}$ and $\tilde{\beta}_{\rm scatt}$ describe the long-distance and long-time fluctuations serving as the scattering sources as discussed throughout the first part of the present section, while $\tilde{\lambda}_b$ and $\tilde{\beta}_b$ represent the microscopic binding force discussed above. In the Appendix B, including $\tilde{\lambda}_b$ and $\tilde{\beta}_b$, it is shown that the center coordinate of a pair of p and q wave packets will simply be accelerated by the external electric field $\boldsymbol{\varepsilon}_s \equiv \boldsymbol{\varepsilon}_p + \boldsymbol{\varepsilon}_q$ added onto them, with an effective mass $m_s = m_p + m_q$ [Eq. (B.7)]. As the relaxation time for p and q are characterized by a single τ_s in (3.24), the corresponding Drude formula will then read $\rho_s = \frac{(m_p+m_q)}{e^2 n \tau_s}$ with

$$\boldsymbol{\varepsilon}_s = \rho_s \mathbf{J}_s^l, \tag{3.31}$$

where $\mathbf{J}_s^l \equiv \mathbf{J}_p^l = \mathbf{J}_q^l$. According to the current constraint (3.8), we find that the electron resistivity, defined by $\boldsymbol{\varepsilon} = \rho \mathbf{J}_e$, has a simple form $\rho = \rho_h + \rho_s$. Since $\rho_h/\rho_s \simeq (\frac{J}{t_h})\frac{k_B T}{t_h} \ll 1$, one therefore obtains the linear-T resistivity

$$\rho \propto k_B T. \tag{3.32}$$

The corresponding relaxation rate is $\hbar/\tau_s \simeq 2k_BT$, in which the coefficient is independent of the coupling strength but with a weak doping dependence (cf. Fig. 5). When $|\omega| \gg k_BT$, one also has $\hbar/\tau_s \propto |\omega|$. All of them agree well with the optical measurements[1] of the high-T_c copper oxide materials. Generally one expects to see a small T^2 upturn in (3.32) from ρ_h at a sufficiently high temperature.

Hall effect. Now apply the external magnetic field $\boldsymbol{a}^{\rm ext}$. $\boldsymbol{a}^{\rm ext}$ will solely act on the h species, since there is no internal transverse gauge field in (3.7) to transfer the effect to p and q species. One may use the kinetic equation to write down the off-diagonal coefficient ρ_{xy}^h for h species in the form $\rho_{xx}^h = \rho_h$ and $\rho_{xy}^h = -\rho_h \omega_H \tau_h$, where the cyclotron frequency ω_H could differ from the bare one $\omega_H^0 = \frac{eB}{cm_h}$ by an enhanced cyclotron mass m_H. This is due to the fact that in the presence of the external magnetic field a wave packet of holon h has to drag the wave packets of the p and q together to go through the cyclotron motion. This drag force cannot cause the p and q species to perform a coherent cyclotron motion but will enhance the effective cyclotron mass of the h species, since p and q are confined in the LLL and thus their effective masses could be very large. Such a big cyclotron mass is in contrast to the longitudinal transport masses discussed before. Note that the electric field can be directly applied to both the p and q species inside their orbitals, which changes the latter into the current-carrying states and, as a consequence, the total longitudinal effects are simply added up in ρ_s as well as in ρ.

The total transport coefficients can be determined as follows. The current $\mathbf{J}_h$ are decomposed into the longitudinal and transverse components as $\mathbf{J}_h = \mathbf{J}_h^l + \mathbf{J}_h^t$, with $\mathbf{J}_h^l = \sigma_{xx}^h \boldsymbol{\varepsilon}_h$, $\mathbf{J}_h^t = \sigma_{xy}^h (\boldsymbol{\varepsilon}_h \times \hat{\mathbf{z}})$. The longitudinal component $\mathbf{J}_h^l$ has to satisfy the current constraint (3.8), i.e., $\mathbf{J}_h^l = \mathbf{J}_s^l$, which determines the strengths of $\boldsymbol{\varepsilon}_h$ and $\boldsymbol{\varepsilon}_s$ through $\boldsymbol{\varepsilon} = \boldsymbol{\varepsilon}_h + \boldsymbol{\varepsilon}_s$. Then simple algebra will lead to the longitudinal resistivity

$$\rho_{xx} = \rho_h + \rho_s/(1 + \cot^{-2}\theta), \tag{3.33}$$

where ρ_h is negligible in comparison to ρ_s as discussed before and the cotangent Hall angle θ defined by $\cot\theta = \rho_{xx}/\rho_{yx}$ is found as

$$\cot\theta = \frac{1}{\omega_H \tau_h} = \alpha T^2 + C, \tag{3.34}$$

with $\alpha = 2\eta' k_B^2/(\hbar \omega_H t_h)$ and the constant C originating from the scattering of h species with impurities. The T^2 law for the cotangent Hall angle in (3.34) fit well[2,4] to the experimental measurements of high-T_c copper oxide materials. Anderson[3] has proposed that a second scattering rate is needed to interpret the experimental data.[4] It was supported by the Zn impurity effect, which causes an extra T-independent contribution in $\cot\theta$.[4] The scattering rate $\hbar/\tau_h$ found in the present work appears naturally in (3.34) to serve as such a second scattering rate. The Hall coefficient R_H can be written as

$$R_H \simeq \frac{1}{nec}\left(\frac{m_p + m_q}{m_H}\right)\frac{\tau_h}{\tau_s} \propto \frac{1}{T}. \tag{3.35}$$

In order to fit the Hall angle data in $YBa_2Cu_3O_{7-\delta}$ (YBCO), it has been found that the cyclotron mass m_H has to be very large, e.g., $m_H \approx 45 m_e$ if $t_h \simeq 8 \times 830$ K.[4] A mechanism for such an enhancement of m_H comes naturally in the present approach.

The longitudinal resistivity ρ_{xx} in (3.33) shows a magnetoresistance effect

$$\frac{\Delta\rho}{\rho} \approx -\cot^{-2}\theta \propto -B^2 T^{-4}, \tag{3.36}$$

which, however, is usually small, e.g., $\cot^{-2}\theta = 4 \times 10^{-4}$ for YBCO at $T = 100$ K (Ref. 4). Nevertheless, the prediction of the magnetoresistance (3.36) should be observable under a careful experimental arrangement with

a stronger magnetic field or at a lower temperature. In obtaining (3.33) and (3.36), we have neglected the reduction of the longitudinal conductivity of p and q under the magnetic field: Even though the external magnetic field cannot be directly applied to the p and q species, the longitudinal conductivity of them still can be reduced (as σ_{xx}^{h} for h) due to the local transverse drag effect from h, which is now having a cyclotron motion under the magnetic field. Such a correction would provide a positive contribution to $\Delta\rho/\rho$ in (3.36) without change the Hall angle in (3.34). A further discussion of all the contributions in the magnetoresistance will be presented elsewhere.

Thermopower. Finally we briefly discuss the thermopower $\mathcal{S} = \mathcal{S}_h + \mathcal{S}_s$. $\mathcal{S}_h$ for the h species gives a small temperature-dependent contribution, but $\mathcal{S}_s$ will be dominant. When the temperature is extrapolated down to zero where the broadening of the Landau level vanishes, $\mathcal{S}_s$ will be simply related to the entropy[35] of p and q species and one finds a Heikes-like formula for $\mathcal{S}_s$:

$$\mathcal{S}_s = \frac{k_B}{e} \ln\left(\frac{1-2\delta}{2\delta}\right), \tag{3.37}$$

which agrees very well with the overall doping dependence in $(La_{1-x}Sr_x)_2CuO_4$,[36] (taking $\delta = 2x$), and other materials.[5] The absence of the spin effect in the thermopower measurements[37] also lends support to the present charge-spin separation picture. The broadening effect is expected to become important with increase of temperature and the corresponding temperature dependence of S_s needs to be further explored.

IV. CONCLUSIONS

Based on the framework developed in Ref. 10, the elementary excitations in the flux-binding phase of the t-J model have been constructed in the present paper. An important lesson we learned from this approach is that the real charge and spin excitations can be quite different from the underlying decomposition scheme, which is implemented to account for the no-double-occupancy constraint in the t-J model.

The charge excitation in the normal state has been shown to be rather simple in structure: A charge-carrying holon always has to drag two auxiliary particles to move together. Each of the auxiliary particles is confined in the lowest Landau level under a fictitious magnetic field in the opposite direction. These auxiliary particles represent the spin frustration effect on the doped holes and provide a scattering mechanism for the transport properties.

Thus, to establish the relevance of the theory with the high-T_c copper oxide materials, the transport properties become a key. In this paper, the normal-state transport decided by Eqs. (3.7a)–(3.7c) has been shown to have the following properties. The resistivity is found to be linear in temperature and is related to a relaxation rate $\hbar/\tau = \eta k_B T$, with $\eta \simeq 2$ independent of the coupling strength. Furthermore, $\hbar/\tau \propto |\omega|$ at $|\omega| > k_B T$ is shown. The Hall coefficient behaves like $1/T$ and the cotangent Hall angle follows a T^2 law, as a consequence that a second scattering rate is involved. When extrapolated to zero temperature, the thermopower has a finite intercept, which exhibits a strong doping dependence as $\frac{k_B}{e}\ln\left(\frac{1-2\delta}{2\delta}\right)$. All of these properties are in good agreement with the transport measurements of the high-T_c copper oxide materials.[1,2,4,5] Therefore, the experimental measurements on the transport properties of the high-T_c materials lend a strong support to the present flux-binding phase in its normal state. Furthermore, a magneto resistance $\propto B^2T^{-4}$ has been predicted for such a system. It would be interesting to measure the temperature dependence of the magnetoresistance in the copper oxide materials so that the relevance of the present theory can be further verified.

ACKNOWLEDGMENTS

The authors would like to thank C. W. Chu, J. Clayhold, T.K. Lee, G. Levine, Y. Y. Xue and J. Yang for the helpful discussions.The present work is supported by the Texas Advanced Research Program under Grant No. 3652182 and by the Texas Center for Superconductivity at the University of Houston.

APPENDIX A: EVALUATION OF $\Lambda(q)$ IN EQ. (3.18)

According to the definition

$$\begin{aligned}\Lambda(q) &= \textstyle\sum_{s's} |\gamma_{s'sq}|^2 \\ &= \textstyle\sum_{s's}\sum_{k'k}\langle s'|k+q\rangle\langle k|s\rangle\langle s|k'\rangle\langle k'+q|s'\rangle \\ &= \textstyle\sum_{k'k}\langle k'+q|\hat{\Pi}_0|k+q\rangle\langle k|\hat{\Pi}_0|k'\rangle,\end{aligned} \tag{A1}$$

in which we introduce the definition

$$\hat{\Pi}_0 = \sum_s |s\rangle\langle s|, \tag{A2}$$

where the summation runs over the states in the LLL. According to Ref. 26, one has

$$\begin{aligned}\Pi_0(r_1, r_2) &\equiv \langle \vec{r}_1|\hat{\Pi}_0|\vec{r}_2\rangle \\ &= (2\pi a_0^2)^{-1}\exp\left[-\left(\frac{1}{4a_0^2}\right)(r_1^2+r_2^2)\right. \\ &\quad \left. +\frac{1}{2a_0^2}(x_1 - iy_1)(x_2+iy_2)\right].\end{aligned} \tag{A3}$$

Then it is straightforward to show

$$\Lambda(q) = \int d^2r d^2r' d^2r_1 d^2r_1' u m_{kk'} \langle k'+q|r\rangle\langle r'|k+q\rangle\langle k|r_1\rangle\langle r_1'|k'\rangle \Pi_0(r,r')\Pi_0(r_1,r_1')$$
$$= (2\pi a_0^2)^{-2} \int d^2r d^2r' \exp[i\vec{q}\cdot(\vec{r}-\vec{r}')] \exp\left[-\frac{1}{2a_0^2}|\vec{r}-\vec{r}'|^2\right]$$
$$= (2\pi a_0^2)^{-1} \exp\left[-\frac{a_0^2 q^2}{2}\right]. \tag{A4}$$

APPENDIX B: THE ROLES OF $\tilde{\lambda}_b$ AND $\tilde{\beta}_b$

For a particle in a uniform magnetic field H (perpendicular to the plane) with the presence of a potential field U, its motion is described by the following equations:[38]

$$\ddot{x} = -\omega_c \dot{y} - \frac{1}{m}\frac{\partial U}{\partial x},$$
$$\ddot{y} = \omega_c \dot{x} - \frac{1}{m}\frac{\partial U}{\partial y}, \tag{B1}$$

which is similar to the classical equation with the cyclotron frequency $\omega_c = \frac{eH}{mc}$.

For a p species, one has $U = U_p = a_0^p + \tilde{\lambda}_b$, while for a q species, $U = U_q = a_0^q + \tilde{\beta}_b$ with $H \to -H$ in (B1). Now suppose an external electric field is applied to the p and q species along y direction such that $a_0^p = -\varepsilon_p y$ and $a_0^q = -\varepsilon_q y$. Without $\tilde{\lambda}_b$ and $\tilde{\beta}_b$, p and q species would go through a transverse motion in the opposite directions of x axis according to (B1). However, $\tilde{\lambda}_b$ and $\tilde{\beta}_b$ will force p and q bound together at a length scale $q_c^{-1} \sim a_0$, which essentially will cancel out such a transverse effect as shown below.

One may write

$$x = x_{cy} + X,$$
$$y = y_{cy} + Y, \tag{B2}$$

where x_{cy} and y_{cy} describe the cyclotron motions of p or q species within a length scale $\sim a_0$ while X and Y represent the motions in a larger scale. In the y direction, the electric forces are given by

$$\frac{\partial U_p}{\partial y} = -\varepsilon_p = \frac{\partial U_p}{\partial Y},$$
$$\frac{\partial U_q}{\partial y} = -\varepsilon_q = \frac{\partial U_q}{\partial Y}. \tag{B3}$$

In the x direction, the binding forces have to be implemented through $\tilde{\lambda}_b$ and $\tilde{\beta}_b$ to cancel out the opposite transverse motions of the p and q particles:

$$\frac{\partial U_p}{\partial x} \approx \frac{\partial \tilde{\lambda}_b}{\partial X} = \frac{\partial U_p}{\partial X},$$
$$\frac{\partial U_q}{\partial x} \approx \frac{\partial \tilde{\beta}_b}{\partial X} = \frac{\partial U_q}{\partial X}. \tag{B4}$$

Here the condition that $\tilde{\lambda}_b$ and $\tilde{\beta}_b$ have a short-distance cutoff at $q_c^{-1} \sim a_0$ has been used. Then x_{cy}, y_{cy} and X, Y can be decoupled as

$$\ddot{x}_{cy} = -\omega_c \dot{y}_{cy},$$
$$\ddot{y}_{cy} = \omega_c \dot{x}_{cy}, \tag{B5}$$

and

$$\ddot{X} = -\omega_c \dot{Y} - \frac{1}{m}\frac{\partial U}{\partial X},$$
$$\ddot{Y} = \omega_c \dot{X} - \frac{1}{m}\frac{\partial U}{\partial Y}. \tag{B6}$$

Equation (B4) describes the unperturbed motions of the p and q species. And X and Y may be interpreted as the center coordinates of the wavepackets of p and q species, which should be bound together, i.e., $X_p = X_q \equiv X$, $Y_p = Y_q \equiv Y$. Note that $\tilde{\lambda}_b$ and $\tilde{\beta}_b$ will force $\dot{X}_p = \dot{X}_q = 0$, Equation (B5) will then reduce to

$$\pm\omega_c \dot{Y} = -\frac{1}{m_{p,q}}\frac{\partial U_{p,q}}{\partial X},$$
$$\ddot{Y} = -\frac{1}{m_{p,q}}\frac{\partial U_{p,q}}{\partial Y}. \tag{B7}$$

From (B6), one can easily find

$$m_s \ddot{Y} = \varepsilon_s - \frac{m_s}{\tau_s}\dot{Y}, \tag{B8}$$

where $m_s = m_p + m_q$ and a dissipation term has been added to the right-hand side of (B7) with the relaxation time τ_s defined in (3.24). The binding fields $\tilde{\lambda}_b$ and $\tilde{\beta}_b$ are determined by the following equations:

$$\frac{\partial^2 \tilde{\lambda}_b}{\partial X \partial t} + \frac{1}{\tau_s}\frac{\partial \tilde{\lambda}_b}{\partial X} = -\varepsilon_s \omega_c \left(\frac{m_p}{m_s}\right),$$
$$\frac{\partial^2 \tilde{\beta}_b}{\partial X \partial t} + \frac{1}{\tau_s}\frac{\partial \tilde{\beta}_b}{\partial X} = \varepsilon_s \omega_c \left(\frac{m_q}{m_s}\right). \tag{B9}$$

Equation (B7) means that beyond a length scale $\sim q_c^{-1}$, p and q particles are bound together and behave simply like a single particle with a mass m_s under a longitudinal electric field.

[1] For a review, see, D. B. Tanner and T. Timusk, in *Physical Properties of High Temperature Superconductors*, edited by P. M. Ginsberg (World Scientific, Singapore, 1992), Vol. 3, p. 363.

[2] For a review, see, N. P. Ong, in *Physical Properties of High Temperature Superconductors* (Ref. 1), Vol. 2, p. 459.

[3] P. W. Anderson, Phys. Rev. Lett. **67**, 2092 (1991).

[4] T. R. Chien, Z. Z. Wang, and N. P. Ong, Phys. Rev. Lett.

67, 2088 (1991).
[5] For a review, see, A. B. Kaiser and C. Uher, in *Studies of High Temperature Superconductors*, edited by A. Narlikar (Nora Science Publishers, New York, 1991).
[6] L. B. Ioffe and A. I. Larkin, Phys. Rev. B **39**, 8988 (1989).
[7] N. Nagaosa and P. A. Lee, Phys. Rev. Lett. **64**, 2450 (1990); Phys. Rev. B **46**, 5621 (1992).
[8] L. B. Ioffe and P. B. Wiegmann, Phys. Rev. Lett. **65**, 653 (1990); L. B. Ioffe and G. Kotliar, Phys. Rev. B **42**, 10 348 (1990).
[9] P. W. Anderson, Phys. Rev. Lett. **64**, 1839 (1990); **65**, 2306 (1990).
[10] Z. Y. Weng, D. N. Sheng, and C. S. Ting, Phys. Rev. B **49**, 607 (1994).
[11] Z. Y. Weng, D. N. Sheng, and C. S. Ting, Phys. Lett. A **175**, 455 (1993).
[12] Z. Y. Weng, D. N. Sheng, C. S. Ting, and Z. B. Su, Phys. Rev. Lett. **67**, 3318 (1991); Phys. Rev. B **45**, 7850 (1992).
[13] P. B. Wiegmann, Phys. Rev. Lett. **65**, 2070 (1990).
[14] Y. Hasegawaw, O. Narikiyo, K. Kuboki, and H. Fukuyama, J. Phys. Soc. Jpn. **59**, 822 (1990).
[15] J. P. Rodriguez and B. Doucot, Phys. Rev. B **42**, 8724 (1990); **45**, 971 (1992).
[16] Z. Zou, J. L. Levy, and R. B. Laughlin, Phys. Rev. B **45**, 993 (1992).
[17] A. M. Tikofsky, R. B. Laughlin, and Z. Zou, Phys. Rev. Lett. **69**, 3670 (1992).
[18] P. Lederer, D. Poilblanc, and T. M. Rice, Phys. Rev. Lett. **63**, 1519 (1989); Y. Hasegawa, P. Lederer, T. M. Rice, and P. B. Wiegmann, *ibid.* **63**, 907 (1989).
[19] S. E. Barnes, J. Phys. F **6**, 1375 (1976); P. Coleman, Phys. Rev. B **29**, 3035 (1984); N. Read and D. Newns, J. Phys. C **16**, 3237 (1983).
[20] V. Kalmeyer and R. B. Laughlin, Phys. Rev. Lett. **59**, 2095 (1987).
[21] R. B. Laughlin, Science **242**, 525 (1988); Phys. Rev. Lett. **60**, 2677 (1988).
[22] J. R. Schrieffer, *Theory of Superconductivity* (Benjamin/Cummings, New York, 1964).
[23] A. L. Fetter, C. B. Hanna, and R. B. Laughlin, Phys. Rev. B **39**, 9679 (1989).
[24] Y. H. Chen, F. Wilczek, E. Witten, and B. I. Halperin, Int. J. Mod. Phys. B **3**, 1001 (1989).
[25] Q. Dai, J. L. Levy, A. L. Fetter, C. B. Hanna, and R. B. Laughlin, Phys. Rev. B **46**, 5642 (1992).
[26] C. B. Hanna, R. B. Laughlin, and A. L. Fetter, Phys. Rev. B **40**, 8745 (1989).
[27] Y. Kitazawa and H. Murayama, Phys. Rev. B **41**, 11 101 (1990).
[28] X. G. Wen and A. Zee, Phys. Rev. B **41**, 240 (1990).
[29] H. Mori, Phys. Rev. B **42**, 184 (1990).
[30] F. Wilczek, *Fractional Statistics and Anyon Superconductivity* (World Scientific, Singapore, 1990).
[31] G. S. Canright, S. M. Girvin, and A. Brass, Phys. Rev. Lett. **63**, 2291 (1989); **63**, 2295 (1989).
[32] C. Kallin, Phys. Rev. B **48**, 13 742 (1993).
[33] C. Gros, S. M. Girvin, G. S. Canright, and M. D. Johonson, Phys. Rev. B **43**, 5883 (191).
[34] Z. Y. Weng, (unpublished).
[35] P. M. Chaikin and G. Beni, Phys. Rev. B **13**, 647 (1976).
[36] J. R. Cooper *et al.*, Phys. Rev. B **35**, 8794 (1987).
[37] R. C. Yu *et al.*, Phys. Rev. B **37**, 7963 (1988).
[38] R. Kubo *et al.* in *Solid State Physics*, edited by F. Seitz and D. Turnbull (Academic, New York, 1965), Vol. 17, p. 270.